Available online at www.CivileJournal.org

Civil Engineering Journal

Vol. 2, No. 4, April, 2016

An Investigation of Local Site Effects Using Linear and Nonlinear Analysis and Comparison between Them

Ali Komak Panah[a] , Aylin Nouri[b*]

[a]Associate Prof., Department of Soil and Foundation Engineering, Faculty of Civil and Environmental Engineering Tarbiat Modares University

[b]M.Sc Student of Geotechnic-Civil Engineering, Department of Soil and Foundation Engineering, Faculty of Civil and Environmental Engineering Tarbiat Modares University

Received 15 March 2016; Accepted 19 April 2016

Abstract

Recent code provisions for building and other structures (1994 and 1997 NEHRP provisions, 1997 UBC) have adopted new site classification. The new site classification system is based on average shear wave velocity to a depth of 30 m. when the shear wave velocity is not available; other soil properties such as undrained shear strength can be used. The study of propagation damages in various earthquakes illustrates the importance of the site effect on the ground seismic characteristics. From the point of the earthquake engineering view, the most important characteristics of the strong ground motion are amplitude, frequency content and duration. All of these properties have a significant effect on earthquake damage. The behavior of soils under cyclic loading is basically nonlinear and hysteretic. Ground response analysis is used to predict the movements of the ground and develop a design response spectrum in order to determine the dynamic stresses and strains and earthquake forces. The profile was studied by using various methods of soil response analysis and finally, the results were examined. In this paper, soil responses were examined by NERA, EERA software and the results compared with each other. Eventually, we concluded that the values obtained from the EERA are more than the value obtained from the NEERA software.

Keywords: EERA; NERA; Site Effect; Ground Response.

1. Introduction

These Earthquakes are caused by sudden slips on geological faults. Seismic waves are then generated and propagate through the lithosphere up to the earth surface. The induced seismic movement depends on the earthquake magnitude (the energy produced by the source), but also on the path followed within the lithosphere (regional hazard) and on local conditions (local hazard). The modification of the seismic movement due to local topographical and geotechnical conditions is called site effect. This amplification or attenuation is obtained by comparing the response of a site with the one of a reference site, i.e. a site located on flat rock. These site effects are mainly observed at the top of hills or in alluvial valleys, where buildings suffer greater damage than might have been expected from their distance to the epicentre. The most famous example of this phenomenon is the 1985 Michoacan earthquake, during which the city of Mexico, located 400 km from the epicentre, was greatly damaged. The maximum acceleration recorded in the valley had been five times higher than at a nearby site located on rock [1, 2].

Methods of analysis of the response of soil deposits during earthquakes are presented. These methods include linear elastic analysis, a nonlinear analysis and an equivalent linear analysis. All these methods require that: (1) the surface of the layer, the interface between any two sublayers and the base of the layer is essentially horizontal, (2) the material properties of the layer are constant along any horizontal plane and (3) the applied seismic excitation is also horizontal [3, 4].

*Corresponding author: ayleen.nouri@modares.ac.ir

2. One-Dimensional Ground Response Analysis in EERA

Detailed one-dimensional ground response analysis is based on the viscoelastic propagation of shear waves in vertical direction through a layered soil deposit over half-space (Tsai and Housner, 1970). The assumption of vertical propagation of waves is expected to be satisfied, because the waves are refracted to a near-vertical direction due to decrease in velocities of surface deposits. The layers are numbered 1 (top layer) to N (half space) with each layer characterized by thickness h_m , mass density ρ_m , shear modulus G_m , and damping ratio ξ_m. For viscoelastic wave propagation, soils are usually modeled as Kelvin-Voigt solids with the following form of stress-strain relationship:

$$\tau = G(1 + 2i\zeta)\gamma = G^*\gamma \quad (1)$$

Where τ is the shear stress, $\gamma = \frac{\partial u}{\partial z}$ is the shear strain, and G^* can be interpreted as a complex shear modulus.
Considering a coordinate system z_m for each layer in vertically downward direction with origin at the top of the layer, the horizontal displacement in the mth layer can written as

$$u(z_m, t)_m = \left(A_m e^{ik^*_m z_m} + B_m e^{-ik^*_m z_m}\right)e^{i\omega t} \quad (2)$$

With $K^{*2} = \frac{\rho\omega^2}{G+i\omega\eta} = \frac{\rho\omega^2}{G^*}$ as the complex wave-number. This can be used to define the strain and stress in the layer. The continuity of displacements and stresses at the layer interfaces results in the following recursive relationships:

$$A_{m+1} = \frac{1}{2}A_m(1 + \alpha^*_m)e^{ik^*_m h_m} + \frac{1}{2}B_m(1 - \alpha^*_m)e^{-ik^*_m h_m} \quad (3)$$

$$B_{m+1} = \frac{1}{2}A_m(1 - \alpha^*_m)e^{ik^*_m h_m} + \frac{1}{2}B_m(1 + \alpha^*_m)e^{-ik^*_m h_m} \quad (4)$$

Where $\alpha^*_m = \frac{k^*_m G^*_m}{k^*_{m+1} G^*_{m+1}} = \sqrt{\frac{\rho_m G^*_m}{\rho_{m+1} G^*_{m+1}}}$ is the complex impedance ratio at the boundary between m and m+1 layers.
The shear stress at the free surface has to be zero, which leads to $A_1 = B_1$. The wave amplitudes in mth layer can thus be expressed in terms of the amplitudes in the top layer by repeated use of the recursive relations in the following functional form:

$$A_m = a_m(\omega)A_1 \ \ and \ B_m = b_m(\omega)B_1 \quad (5)$$

The transfer function relating the displacement amplitude at ith layer to that at jth layer can thus be defined by

$$F_{ij}(\omega) = \frac{|u_i|}{|u_j|} = \frac{A_i + B_i}{A_j + B_j} = \frac{a_i(\omega) + b_i(\omega)}{a_j(\omega) + b_j(\omega)} \quad (6)$$

Since $|\dot{u}(z,t)| = \omega\,|u(z,t)|$ and $|\ddot{u}(z,t)| = \omega^2\,|u(z,t)|$for harmonic motion, this also describes the amplification of velocities and accelerations from ith to jth layer. Thus the motion in any layer can be determined from the motion in any other layer. The shear modulus, G, and damping ratio, ξ, depend on the shear strain in a nonlinear manner, with G decreasing and ξ increasing with increase in the level of strain. Laboratory testing is necessary to define accurately the strain dependence of G and ξ for each soil layer, which may not always be possible. Therefore, standard curves from published literature for different types of soil in terms of the maximum values of G are used commonly in real practice (Vucetic and Dobry, 1991). The exact time-history solution of the wave equation to consider accuratelythe nonlinear soil behavior is highly cumbersome and time taking. An equivalent linear method using aniterative procedure is therefore used commonly in practical applications. In this method, for a given input acceleration time-history, the time-history of shear strain in each soil layer is computed using the foregoing formulation for selected fixed initial values of G and ξ (e.g., zero strain values). By taking the effective strain in each layer to be $\frac{(M-1)}{10}$ times the estimated maximum shear strain γ_{max}, where M is the earthquake magnitude, the new equivalent linear values of G and ξ are obtained from the modulus reduction and the damping curves for the effective strain value. This process is iterated till the input values of G and ξ are consistent with the estimated effective shear strain.
The SHAKE is the earliest software written to implement the equivalent linear method (Schnabel et. al., 1972), which has been updated many times, with SHAKE91 being the most recent version (Idriss and Sun, 1992). This has been by far the most widely used program for computing seismic response of horizontally layered soil deposits. Program EERA was developed in FORTRAN90 from this basic code to take full advantage of the dynamic array dimensioning and matrix operations (Bardet et al., 2000). EERA's input and output are integrated with the spreadsheet program Excel [5-7].

2.1. Main features of EERA

- EERA dynamic library is implemented in FORTRAN 90. All matrix and vector calculations are performed without indices. One of the main advantages of FORTRAN 90 over its predecessors is the dynamic dimensioning

of arrays. The size of the arrays adapt to the size of the problems, within the limit of the computer available memory. EERA dimensions internally its work arrays depending on the problem size.

- As a benefit of dynamic dimensioning, there is no limit on the total number of material properties and soil layers in EERA
- As another benefit of dynamic dimensioning, the users can prescribe the number of data points for FFT beyond 4096. Larger numbers of data points are useful to describe high frequencies in the calculations. However, longer computation times are likely to result from larger number of data points in the FFT calculations.
- The relative displacement and velocity can be calculated in sublayers.
- The users can select calculations for a filtered or unfiltered object motion.
- EERA uses an optimized version (IMSL, 1998) of the Cooley and Tukey algorithm for FFT [7].

3. One-Dimensional Ground Response Analysis in NERA

Figure 1 schematizes the geometry and boundary conditions of one-dimensional site response analysis. Shear waves propagate vertically in a one-dimensional layered system, in which the soil layers are assumed to be (1) horizontally homogenous, (2) of infinite horizontal extent, and (3) subjected only to horizontal motion from bedrock. The governing equation is:

$$\rho \frac{\partial^2 d}{\partial t^2} + \eta \frac{\partial d}{\partial t} = \frac{\partial \tau}{\partial z} \tag{7}$$

Where ρ is the soil unit mass; d is the horizontal displacement; z is the depth; t is the time; τ is the shear stress; and η is a mass-proportional damping coefficient. The boundary conditions are specified at the free surface (z = 0) and at the bottom of the soil column (i.e., z = H):

$$\tau = 0 \ at \ z = 0 \ \ and \ \ \tau = \tau_B \ \ at \ \ z = H \tag{8}$$

The shear stress τ_B at z = H, which is usually unknown, is calculated from the velocity at z = H.

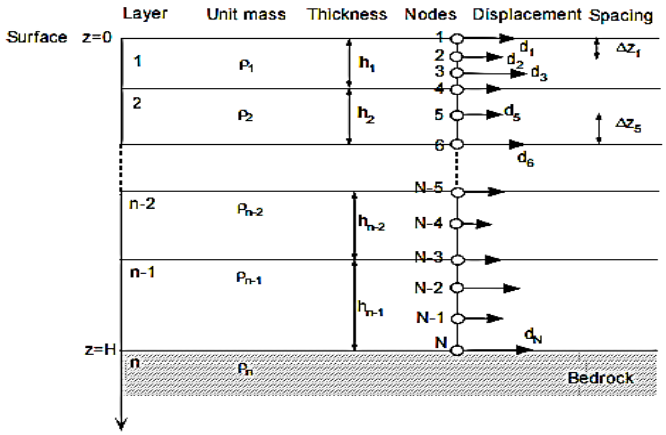

Figure 1. One-dimensional layered soil deposit system and its spatial discretization [8, 9]

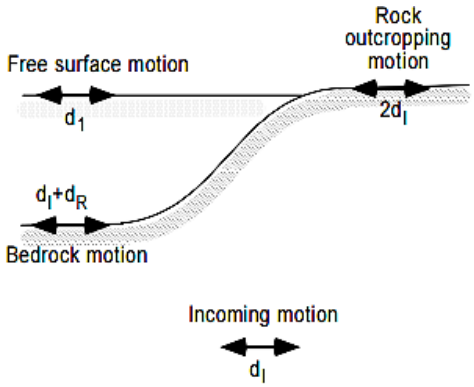

Figure 2. Terminology used in site response analysis, and shear wave amplitude at various [9]

As shown in Figure 2, the earthquake generates an incoming shear wave which propagates vertically upward and has for amplitude d_I through the bedrock. The wave amplitude is $d_I + d_R$ at the top of the bedrock under the soil layers where d_R is the amplitude of the wave refracted at the soilbedrock interface. The wave amplitude is 2 d_I at the rock outcrop because there is no shear stress on free surfaces. The wave amplitude d_1 at the top of the soil column is the main quantity to be determined by site response analysis. The stress τ_B at the bottom of the soil column (z = H)

can be calculated assuming that the bedrock is elastic. Incident waves travel upward through a rock with shear wave velocity v_s. The particle displacement d_I due to the incident wave in the bedrock is a function of depth z and time t:

$$d_I = d_I(z + v_s t) \tag{9}$$

Similarly, the particle displacement d_R due to the reflected wave at the soil-bedrock interface is:

$$d_R = d_R(z - v_s t) \tag{10}$$

The shear stress τ_B is:

$$\tau_B = \mu\left(\frac{\partial d_I}{\partial z} + \frac{\partial d_R}{\partial z}\right) \tag{11}$$

Where μ is the shear modulus of the bedrock. Taking the first derivative of Eqs. 9 and 10,

$$\frac{\partial d_I}{\partial z} = \frac{v_I}{v_s} \quad \text{and} \quad \frac{\partial d_R}{\partial z} = -\frac{v_R}{v_s} \tag{12}$$

Where v_I and v_R are the particle velocity of the incident and refracted waves, respectively. The velocity v_B at z = H is the sum of the velocity of incident and reflected waves,

$$v_B = v_I + v_R \tag{13}$$

Using Eqs. 11 to 12, τ_B becomes,

$$\tau_B = \frac{\mu}{v_s}(2v_I - v_B) = \rho v_s(2v_I - v_B) \tag{14}$$

Where ρ is the unit mass of the bedrock. Equation 14 relates the shear stress and velocity at the soil-column interface; it provides an additional equation to define the shear stress at the lower boundary. Equation 14 also applies to the case of rock outcropping: since $\tau_B = 0$ then $v_B = 2\, v_I$ [9-12].

3.1. Finite Difference Formulation of One-Dimensional Site Response Analysis

3.1.1. Spatial and Time Discretization

As shown in Figure 1, the soil deposit is divided into m-1 layers having various thickness h_i and unit mass ρ_i for i = 1 to m-1. The displacement d and stress τ are evaluated at N grid nodes, which define sublayers within layers. The displacement of node i at time t_n is denoted $d(z_i , t_n) = d_{i,n}$where z_i is the depth of node i. Similarly the stress and strain at node i at time t_n are denoted $\tau_{i,n}$ and $\gamma_{i,n}$, respectively. $v_{i,n}$ and $a_{i,n}$. denote the velocity $v(z_i , t_n)$ and acceleration $a (z_i , t_n)$ of node i at time t_n. First order derivative are approximated using a forward finite-difference approximation:

$$\frac{df(z_i)}{dz} = \lim_{\Delta z_i \to 0} \frac{f(z_{i+1}) - f(z_i)}{\Delta z_i} \tag{15}$$

where f represents any differentiable function and $\Delta z_i = z_{i+1} - z_i$. Forward finite-difference is preferred to higher order approximation because it accounts simply for the discontinuity of displacement derivatives at the layer interfaces. The strain (i.e., displacement gradient) in the layer below node i and time t_n is:

$$\gamma_{in} = \frac{\partial d}{\partial z} = \frac{d_{i+1,n} - d_{i,n}}{\Delta z_i} \tag{16}$$

As shown in Figure 3, strain is constant between nodes i and i+1, which implies that the stress is also constant between nodes i and i+1. The governing equations at nodes i = 1, …, N at time t_n are:

$$\rho_i a_{i,n} + \eta_i v_{i,n} = F_{i,n} \tag{17}$$

where ρ_i and η_i are the unit mass and viscosity of between nodes i and i+1, respectively, and $F_{i,n}$ is the stress gradient at node i. The stress gradient at node i = 2, …, N-1 at time t_n is evaluated as follows:

$$F_{i,n} = \left\{\frac{\partial \tau}{\partial z}\middle| i, n\right\} \approx 2\frac{\tau_{i,n} - \tau_{i-1,n}}{\Delta z_i + \Delta z_{i-1}} \tag{18}$$

At node 1 (surface), the stress should be equal to 0. As shown in Figure 4a, a fictitious node 0 and fictitious layer of thickness Δz_1 are introduced above node 1. In this fictitious layer, the stress $\tau_{0,n}$ should be equal to $-\tau_{1,n}$ so that the average stress is equal to zero at node 1 (i.e.,$\tau_{0,n} + \tau_{1,n=0} = 0$), which implies that:

$$F_{1,n} = \frac{2\tau_{1,n}}{\Delta z_1} \quad (19)$$

At node N (bottom), the stress should be equal to τ_B . As shown again in Figure 4b, a fictitious node N+1 and fictitious layer of thickness Δz_{N-1} are introduced below node N. In this fictitious layer, the stress $\tau_{N,n}$ is equal to $2\tau_{B,n} - \tau_{N-1,n}$, so that the average stress at node N is equal to $\tau_{B,n}$. The stress gradient at node N is therefore:

$$F_{N,n} = \frac{\tau_{N,n} - \tau_{N-1,n}}{\Delta z_{N-1}} = 2\frac{\tau_{B,n} - \tau_{N-1,n}}{\Delta z_{N-1}} \quad (20)$$

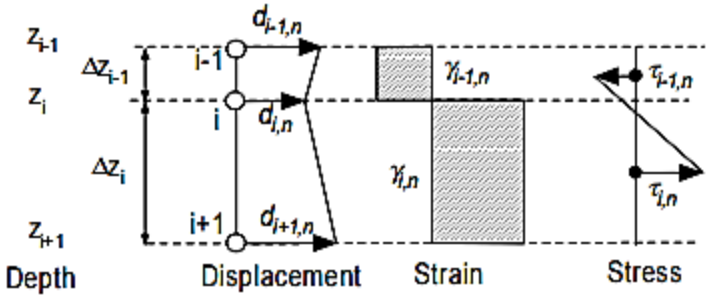

Figure 3. Definition of displacement, strain, and stress in finite-difference formulation [9]

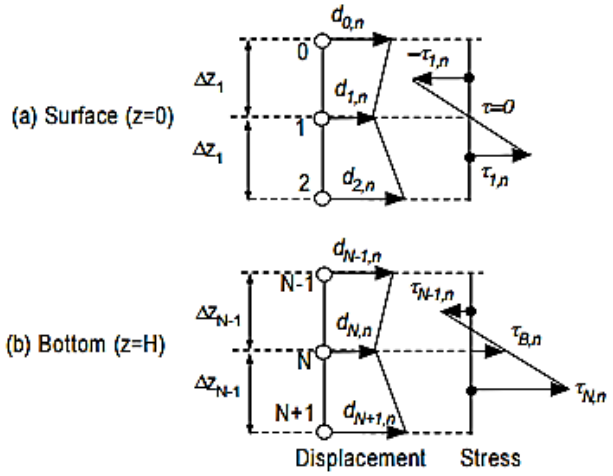

Figure 4. Definition of fictitious nodes 0 and N+1 at (a) surface and (b) bottom of soil [9]

4. Input Parameters

4.1. Earthquake Data

The input motion is specified as an outcrop motion from the acceleration time history recorded during the Manjil-Iran earthquake. Maximum Acceleration is 0.496g at time t=12.32 sec that the ground motion is normalized to a target peak acceleration of 0.496 g. Figure 5 presents the used accelerographs in this paper.

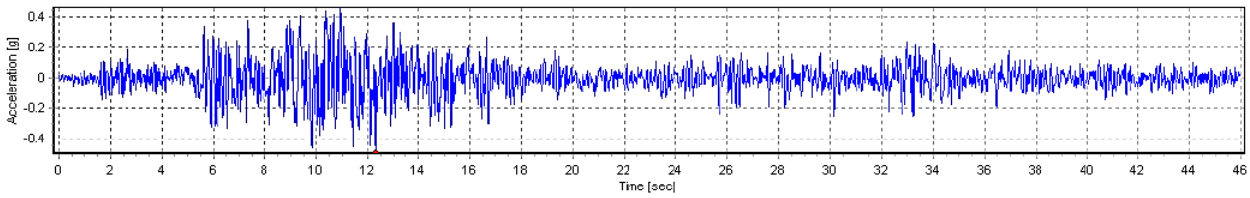

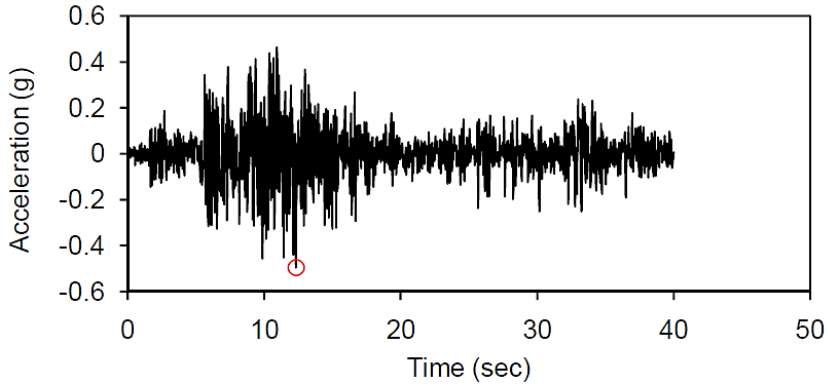

Figure 5. Acceleration time history during the Manjil-Iran earthquake

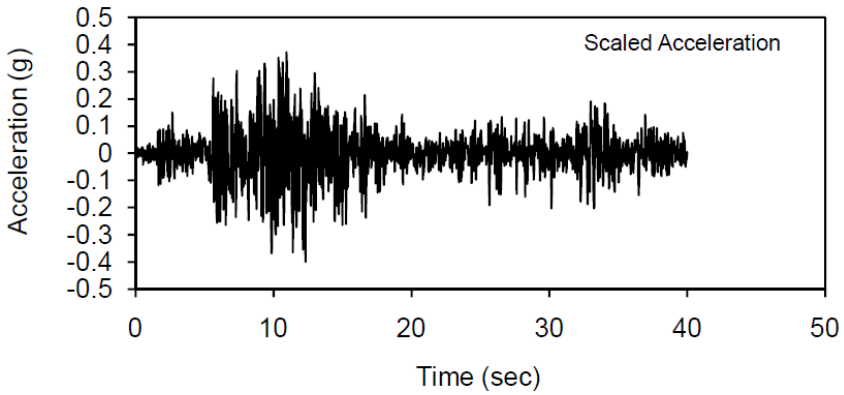

Figure 6. Scaled Acceleration time history during the Manjil-Iran earthquake

4.2. Soil Profile

Because of that seismic waves pass from dozens of kilometres of rock and often less than 100 m of soil, Soil layer, plays a very important role in determining the properties of ground motions. In this paper, soil profile is a 32-m consisting of clay and sand overlying a half-space. The study site is located about 80 kilometres southeast of Tabriz. The Location of the drilled boreholes at the plan map is shown in Figure 7. Table 1 presents the variation of section, shear wave velocity, and total unit weight of different layers of the soil profile. This Soil profile is divided into 17 layers with variable shear wave velocity and unit weight and Figure 8 present the generated G/G0-γ and D-γ for layers of soil profile.

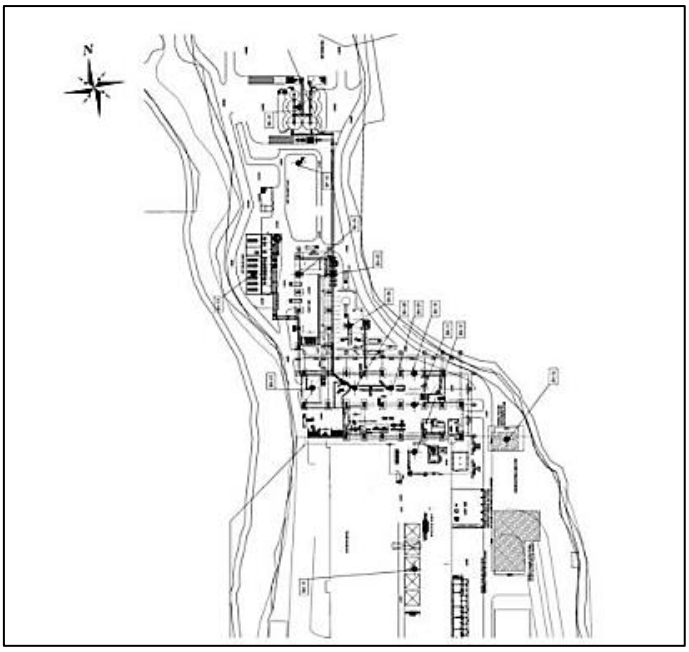

Figure 7. Location of the drilled boreholes at the plan map

Figure 8. Location of the drilled boreholes at aerial map

Table 1. Description of Soil profile

Fundamental period (s) = 0.26
Average shear wave velocity (m/sec) = 500.50
Total number of sublayers = 17

	Layer Number	Soil Material Type	Number of sublayers in layer	Thickness of layer (m)	Maximum shear modulus G_{max} (MPa)	Initial critical damping ratio (%)	Total unit weight (kN/m^3)	Shear wave velocity (m/sec)	Location and type of earthquake input motion	Location of water table	Depth at middle of layer (m)	Vertical effective stress (kPa)
Surface	1	2		1.0	38.99		17.00	*150*			0.5	8.50
	2	2		1.0	50.08		17.00	*170*			1.5	25.50
	3	2		1.0	95.70		17.00	*235*			2.5	42.50
	4	2		1.0	90.31		17.50	*225*			3.5	59.75
	5	1		1.0	125.27		17.50	*265*			4.5	77.25
	6	1		1.0	177.01		17.50	*315*			5.5	94.75
	7	1		1.0	212.33		17.50	*345*			6.5	112.25
	8	1		1.0	237.66		17.50	*365*			7.5	129.75
	9	2		2.0	271.33		17.50	*390*			9.0	156.00
	10	2		2.0	353.26		17.50	*445*			11.0	191.00
	11	2		2.0	402.49		17.50	*475*			13.0	226.00
	12	2		4.0	501.10		17.50	*530*			16.0	278.50
	13	2		4.0	650.79		17.50	*604*			20.0	348.50
	14	2		4.0	784.55		18.50	*645*			24.0	420.50
	15	2		4.0	884.88		18.50	*685*			28.0	494.50
	16	2		2.0	1018.77		18.50	*735*			31.0	550.00
Bedrock	17	0			1372.98	1	21.68	*788.2*	Outcrop		32.0	568.50

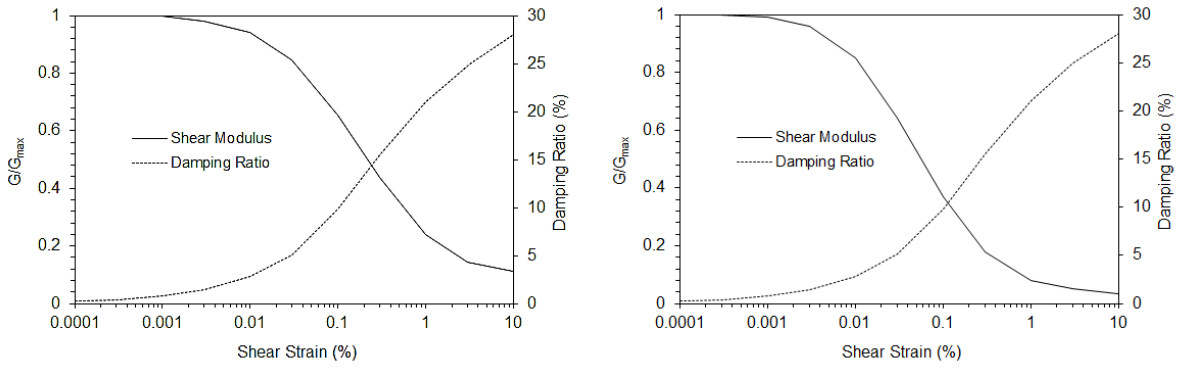

a) b)

Figure 9. Modulus reduction and damping ratio curves a) Clay b) Sand

5. Comparison of NERA and EERA Results

We compare acceleration response spectrum at the free surface with 5% critical damping ratio, transfer function between surface and bedrock and acceleration response spectrum between surface and bedrock that calculated by NERA and EERA. As shown in the figure 11, the magnification of the soil in EERA is about 3 and NERA is 13 also

as shown in the figure 10, maximum acceleration response at the free surface in EERA is 3.7 and in NERA is 2.7. The comparisons showed that Response spectral accelerations calculated for damping ratio of 5% by EERA is more than NERA and the value of the magnification of the soil in EERA is less than NERA, also Comparison of maximum shear strain, maximum shear stress and maximum acceleration along the depth between NERA and EERA showed that is relatively little difference between them. Comparison of the Response spectral accelerations that calculated for damping ratio of 5%, show that the response of the structures on the Surface are more severe than Bedrock, particularly at higher frequencies.

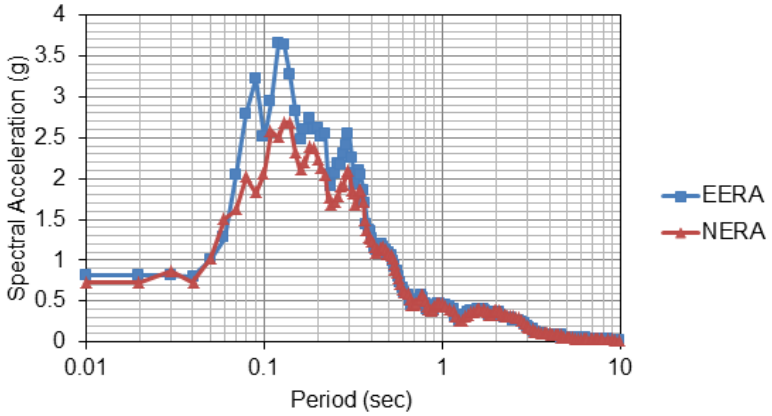

Figure 10. Comparison of Acceleration Response Spectra Calculated by NERA and EERA

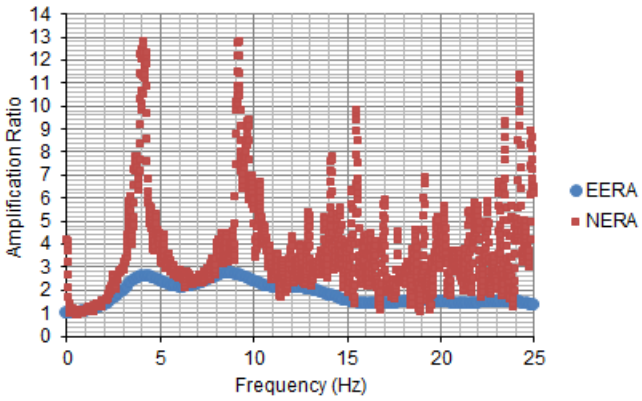

Figure 11. Comparison of transfer function between surface and bedrock calculated by NERA and EERA

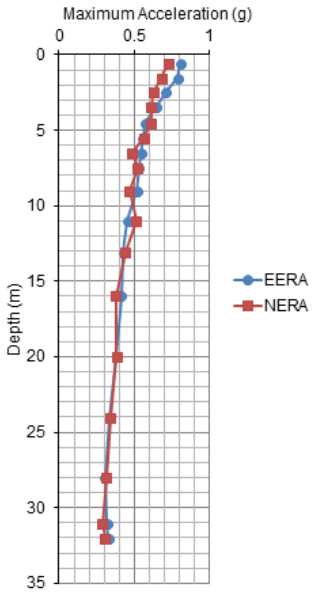

Figure 11. Variation with depth of maximum acceleration

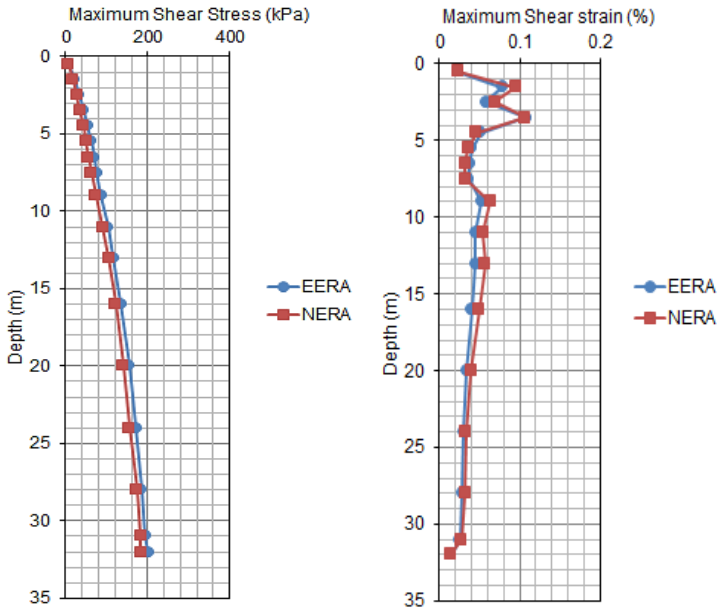

Figure 12. Relative difference of Maximum Shear Stress and Maximum Shear Strain

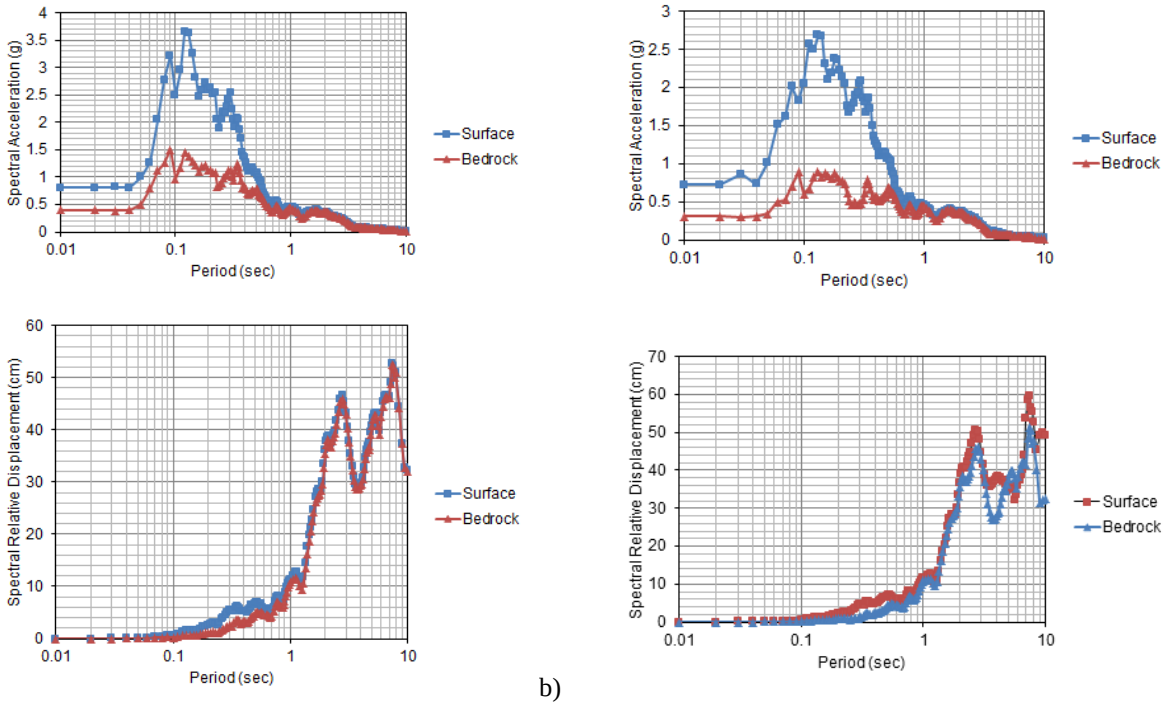

a) b)

Figure 13. acceleration Response Spectra and Displacement calculated by: a) EERA b) NERA

6. Conclusion

The study of propagation damages in various earthquakes illustrates the importance of the site effect on the ground seismic characteristics. Methods of analysis of the response of soil deposits during earthquakes include linear elastic analysis, a Nonlinear analysis and an equivalent linear analysis these methods include the following assumptions:
(1) The surface of the layer, the interface between any two sub-layers and the base of the layer is essentially horizontal, (2) the material properties of the layer are constant along any horizontal plane and (3) the applied seismic excitation is also horizontal. The ground motions on soft soil sites were found to be generally larger than those of nearby rock outcrops, depending on local soil conditions. Response spectral accelerations calculated for damping ratio of 5%, show that the response of the structures on the Surface are more severe than Bedrock, particularly at higher frequencies. For this earthquake, there is relatively little difference between EERA and NERA, but the values obtained from the EERA are more than the value obtained from the NEERA software. Responses of the NEERA software are Nonlinear and closer to the reality, but the EERA software which is used in this paper is linear. In general, Non-Linear method gives lower amounts of the acceleration, velocity and displacements.

7. References

[1] Hashash, Y.M.A., D. Park, and j. lee, "Non-Linear Site Response Analysis for Deep Deposits in the New Madrid Seismic Zone,"International Conferences on Recent Advances in Geotechnical Earthquake Engineering and Soil Dynamics, (2001): p. 7.

[2] Le Pense, Solenn, Behrouz Gatmiri, and Pooneh Maghoul. "Influence of soil properties and geometrical characteristics of sediment-filled valleys on earthquake response spectra." In 8th International Conference on Structural Dynamics (EURODYN 2011, pp. 130-136. 2011.

[3] Biglari, M., and I. Ashayeri. "Seismic ground response analysis of unsaturated soil deposits." Int. J. Civil Eng 11, no. 2 (2013): 150-155.

[4] Idriss, I.M.a.S., H.B., "Seismic response of Horizontal Soil Layers,". Journal ofThe Soil Mechanics and Foundation Division,ASCE, (1968). 94(4): p. 1003-1031.

[5] Ince, G. Ç., and L. Yılmazoğlu. "Investigating the influence of topographic irregularities and two-dimensional effects on surface ground motion intensity with one-and two-dimensional analyses." Natural Hazards and Earth System Science 14, no. 7 (2014): 1773-1788.

[6] Jain, Suman, and I. D. Gupta., "Investigation of Commonly Used Theoretical Methods For Modelling of Soil Amplification Effects", in ISET GOLDEN JUBILEESYMPOSIUM. (2012).

[7] Bardet, J. P., K. Ichii, and C. H. Lin. EERA: a computer program for equivalent-linear earthquake site response analyses of layered soil deposits. University of Southern California, Department of Civil Engineering, 2000.

[8] d’ Avila, Maria Paola Santisi, Jean‐François Semblat, and Luca Lenti. "Strong Ground Motion in the 2011 Tohoku Earthquake: A One‐Directional Three‐Component Modeling." Bulletin of the Seismological Society of America 103, no. 2B (2013): 1394-1410.

[9] Bardet, J. P., and T. Tobita. "A Computer Program for Non-linear Earthquake Response Analyses of Layered Soil Deposits." Department of Civil Engineering, University of Southern California (2001).

[10] Moghaddam, A. Bazrafshan, and M. H. Bagheripour. "Ground response analysis using non-recursive matrix implementation of hybrid frequency-time domain (HFTD) approach." Scientia Iranica 18, no. 6 (2011): 1188-1197.

[11] Effendi, Mahmud Kori, and Eren Uckan. "True nonlinear seismic response analyses of soil deposits." Procedia Engineering 54 (2013): 387-400.

[12] Bagheripour, M. H., M. Asadi, and M. Ghasemi. "Analysis of nonlinear seismic ground response using adaptive nero fuzzy inference systems [J]." Journal of Basic and Applied Scientific Research 2, no. 4 (2012): 3839-3843.